Analysis of the "Crack Characteristic Signal" Using a Generalized Scattering Matrix Representation

Christian Huber, Habibollah Abiri, Stoyan I. Ganchev, *Senior Member, IEEE*, and Reza Zoughi, *Senior Member, IEEE*

***Abstract*— Electromagnetic properties of a system formed by an open-ended rectangular waveguide and a surface crack/slot in a metallic specimen are described in this paper. Scanning a crack on a metal surface changes the reflection coefficient of the incident dominant mode. A model as a function of relative crack location within the waveguide aperture (i.e., crack moving with respect to the waveguide aperture) is desired to describe and optimize practical crack detection applications. Hence, the change in the reflection coefficient for a generalized system encompassing empty, filled, and finite cracks located at an arbitrary position inside the waveguide aperture, is evaluated. A moment solution approach is employed, and a magnetic current density M is introduced over the common aperture formed by the waveguide and the crack. Subsequently, the junction formed by the waveguide and the cracked metallic surface is separated into two systems. A numerical solution employing the method of moments is obtained, and the reflection coefficient at the waveguide aperture is expressed in terms of the generalized scattering matrix. The convergence behavior is studied to determine an optimized set of basis functions and the optimal number of higher order modes for a fast and accurate solution. Numerical results presented in this paper include the evaluation of the field distribution over the waveguide aperture. Finally, the theoretical and measured *crack characteristic signals* are compared.**

***Index Terms*— Microwave crack detection, microwave nondestructive testing, open-ended rectangular waveguide.**

I. Introduction

CURRENTLY, several conventional, nondestructive testing methods are available for detecting surface cracks on metals. acoustic emission testing (AET), dye penetrant testing (PT), eddy current testing (ET), ultrasonic testing (UT), radiographic testing (RT) using x- or gamma radiation, magnetic particle testing (MT), laser shearography, pulsed video thermography (PVT), endoscopy, and optical pattern recognition are examples of these techniques [1]. A few of these techniques are industry's standard for stress and fatigue crack detection. These techniques posses their respective advantages and disadvantages. Nevertheless, research to further increase the sensitivity and effectiveness of these techniques is an ongoing process. These techniques have many shortcomings, particularly when applied to filled and covered cracks [2]. Several researchers have attempted to use microwaves for surface-crack detection [5]–[9]. They utilized different approaches, including mode conversion, planar line sensors, and ferromagnetic resonance probes. A short discussion about the advantages and disadvantages of these methods is presented in [3].

Recent research in using open-ended waveguides for microwave surface-crack detection and sizing have generated much renewed interest in this area [3], [10]–[12]. The microwave technique proposed here (whose foundation has been laid earlier [3], [4]) possesses certain unique features that, once exploited, can advance the state-of-the-art of surface-crack detection. First, the method described in this paper is applicable to both ferromagnetic and nonferromagnetic metals, since this microwave method depends on perturbations in surface currents. Second, the presence of dielectric fillers such as dirt, rust, paint, etc., changes the electrical depth of a crack, but nevertheless they remain readily detectable. Also, cracks covered with thin dielectric coatings such as paint and corrosion-preventative substances are detectable. Third, this microwave method has the potential for remote (noncontact) surface-crack detection (i.e., by introducing an air gap between the waveguide and surface of the metal). A thorough analysis of the change of the reflection coefficient of the dominant mode provides a means for both detecting cracks and evaluating geometrical information such as crack depth, width, and length. It is also possible to determine the crack tip location (the distance between the tips of the crack is its length) of a crack accurately, which is important for repair purposes [13]. A comprehensive discussion of the capabilities of this approach and the optimization possibilities for enhanced crack detection sensitivity are given in [14].

In previous research a mode-matching approach was used to analyze the electromagnetic properties of a system formed by an open-ended waveguide and a crack, and to calculate the *crack characteristic signal* [4], [12]. Subsequently, a distinction between empty, filled (with a dielectric), and finite (i.e., shorter than the broad waveguide dimension) cracks, dependent on the relative position of the crack within the probing waveguide aperture (i.e., in the middle or at the edge), was necessary. A more versatile formulation for eval-

Manuscript received December 12, 1995; revised December 24, 1996. This work was supported in part by the MTT-S 1994 Graduate Fellowship Award presented to C. Huber and in part by the Federal Highway Administration Contract DTFH61-94-X-00023.

C. Huber, S. I. Ganchev, and R. Zoughi are with the Applied Microwave Nondestructive Testing Laboratory (*amntl*), Department of Electrical Engineering, Colorado State University, Fort Collins, CO 80523 USA.

H. Abiri is with the Applied Microwave Nondestructive Testing Laboratory (*amntl*), Department of Electrical Engineering, Colorado State University, Fort Collins, CO 80523 USA, on leave from Shiraz University, Shiraz, Iran.

Publisher Item Identifier S 0018-9480(97)02534-9.

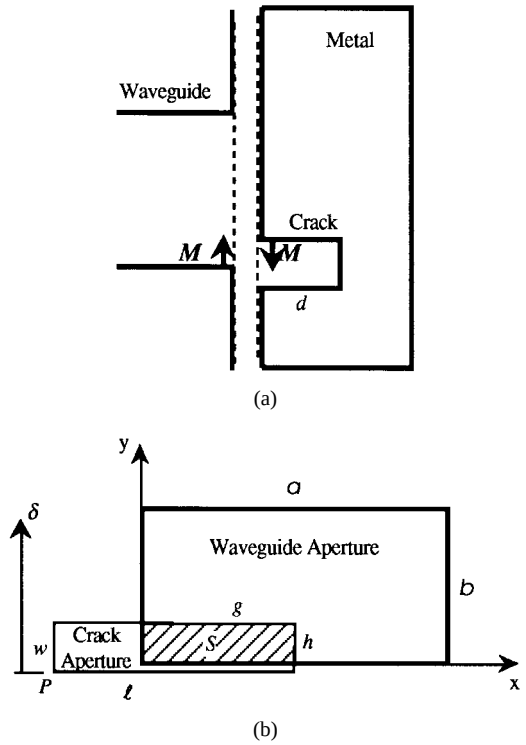

Fig. 1. Relative geometry of a surface crack, a waveguide aperture, and the coordinate system: (a) side view, (b) plan view (at $z = 0$).

uating the electromagnetic properties of such a system is the purpose of this paper. This paper presents a general model for theoretically studying the interaction of an open-ended rectangular waveguide with an open surface crack. The reflection coefficient at the waveguide aperture can be expressed by a generalized scattering matrix, which can be derived by using a moment solution approach [15]. This approach is general and no distinction between exposed, filled, long, and finite cracks is necessary. Furthermore, the approach is independent of the crack position, be it in the middle or at the edge of the waveguide aperture.

Fig. 1(a) and (b) show the relative geometry of a crack with width w, depth d, length ℓ, and an open-ended waveguide with dimensions a and b when the crack length is parallel to the broad dimension of the waveguide. A rectangular slot is the approximation to an open surface hairline crack used in this development. A maximum perturbance of the surface currents occurs for this geometry [Fig. 1(a) and (b)]. In reality, fatigue/hairline cracks are not exactly straight, but they have a preferred direction of propagation. Nevertheless, as long as the crack is not orthogonal to the broad dimension of the waveguide (i.e., aligned with the incident electric-field vector) it can still be detected. The scanning distance δ indicates the position of the crack relative to an arbitrary location on the narrow dimension of the waveguide aperture b. The *crack characteristic signal* refers to the detector (used to sense the standing wave inside the waveguide away from the aperture) voltage variations as a function of scanning distance δ, obtained when a crack is scanned over a waveguide aperture [3]. A rapid change in the phase of the reflection coefficient occurs when the crack moves over the edge of the waveguide aperture while the phase of the reflection coefficient remains fairly constant when the crack is within the middle of the waveguide aperture [3]. An analysis of the *crack characteristic signal* allows one to obtain information about the physical dimensions of the crack, as each signal is unique to the crack geometry and the operating frequency.

II. System Description

In order to obtain a general representation of a system formed by a waveguide aperture and a metallic surface with a crack, arbitrary incident electric and magnetic fields in the waveguide are assumed. The incident and reflected fields in the waveguide and the crack are expressed in terms of their discrete orthonormal eigenfunctions (for the dominant mode and the higher order modes) with unknown complex coefficients. These coefficients represent the amplitude and the phase of the respective eigenfunctions. A magnetic current density $\boldsymbol{M}$ is introduced over the common aperture (of the system) formed by the waveguide and the crack (Fig. 1). This system can then be separated into two parts [16]. It must be noted that in this approach an analysis of the electromagnetic properties as a function of the relative crack location within the waveguide aperture is needed. This means that it is necessary to evaluate the change of reflection coefficient as the crack is being scanned (i.e., the crack location is continuously varying within the waveguide aperture). That includes the crack being partially outside in either x- or y-directions. Applying the method of moments provides for a numerical solution for the complex field coefficients [17]. The accuracy of approximating the electric- and magnetic-field distributions anywhere in the waveguide, or in the crack, subsequently depends upon the number of higher order modes used, and it depends on the appropriate choice of the basis functions for the method of moments. The convergence behavior is then used for analyzing all of these criteria. Finally, a generalized scattering matrix is formulated by writing the system of equations in a matrix form and solving for the reflection coefficient at the aperture of the waveguide [18]. The input parameters of the theoretical model are the crack dimensions, waveguide aperture dimensions, frequency of operation, and dielectric constant of the material filling the crack. In addition, for the evaluation of the *crack characteristic signal*, the scanning step width is also needed.

III. Formulation of the Generalized Scattering Matrix

The fields in the waveguide and the crack are represented by their orthonormal mode vectors which form complete sets for describing the respective electromagnetic fields [2], [19]–[20]. By normalization, the power is divided between modes according to the square of its amplitudes [21]. The ith orthonormal mode vectors for the waveguide side (index a) are given by $\boldsymbol{e}_{ai}^{\mathrm{TE}}$, $\boldsymbol{h}_{ai}^{\mathrm{TE}}$, $\boldsymbol{e}_{ai}^{\mathrm{TM}}$, and $\boldsymbol{h}_{ai}^{\mathrm{TM}}$. For the crack side (index b) the orthonormal mode vectors $\boldsymbol{e}_{bi}^{\mathrm{TE}}$, $\boldsymbol{h}_{bi}^{\mathrm{TE}}$, $\boldsymbol{e}_{bi}^{\mathrm{TM}}$, and $\boldsymbol{h}_{bi}^{\mathrm{TM}}$ are given in a similar fashion by taking the appropriate physical dimensions into account (replacing a with $b\ell$ and with w, respectively).

The orthonormal mode vectors satisfy the orthogonality relationship in the waveguide and in the crack, respectively. The fields in the waveguide and the crack are well defined by the solutions of Maxwell's equations which satisfy all the boundary conditions except at the junction. Forcing the boundary conditions for the transverse fields at the aperture allows one to effectively solve for all the unknown field coefficients.

A. The Equivalence Principle

The system formed by the waveguide and the crack is divided into two parts (for a generalized representation) using the equivalence principle. The equivalence principle states that the fields in the waveguide are identical to the excitation fields plus the fields produced by an equivalent magnetic current density $\boldsymbol{M}$ when the aperture S is replaced by a perfect conductor [16]. In the crack, the total field is composed of two components resulting from the reflection by the short-circuited end of the crack plus the field produced by the equivalent magnetic current density $-\boldsymbol{M}$ over the aperture S, as shown in Fig. 1.

Hence, the total transverse electric and magnetic fields in the waveguide (index a) are now given by

$$\boldsymbol{E}_{at} = \sum_i C_i e^{-\gamma_{ai} z} \boldsymbol{e}_{ai} - \sum_i C_i e^{\gamma_{ai} z} \boldsymbol{e}_{ai} + \sum_i D_i e^{\gamma_{ai} z} \boldsymbol{e}_{ai} \tag{1a}$$

$$\boldsymbol{H}_{at} = \sum_i C_i Y_{ai} e^{-\gamma_{ai} z} \boldsymbol{u}_z \times \boldsymbol{e}_{ai} + \sum_i C_i Y_{ai} e^{\gamma_{ai} z} \boldsymbol{u}_z \times \boldsymbol{e}_{ai} - \sum_i D_i Y_{ai} e^{\gamma_{ai} z} \boldsymbol{u}_z \times \boldsymbol{e}_{ai}. \tag{1b}$$

Here C_i and D_i are the respective coefficients of the incident modes and the modes produced by $\boldsymbol{M}$. In the crack (index b) the total transverse fields are then given by

$$\boldsymbol{E}_{bt} = \sum_i B_i e^{-\gamma_{bi} z} \boldsymbol{e}_{bi} - \sum_i B_i e^{\gamma_{bi} z} \boldsymbol{e}_{bi} + \sum_i G_i e^{-\gamma_{bi} z} \boldsymbol{e}_{bi} \tag{2a}$$

$$\boldsymbol{H}_{bt} = \sum_i B_i Y_{bi} e^{-\gamma_{bi} z} \boldsymbol{u}_z \times \boldsymbol{e}_{bi} + \sum_i B_i Y_{bi} e^{\gamma_{bi} z} \boldsymbol{u}_z \times \boldsymbol{e}_{bi} + \sum_i G_i Y_{bi} e^{-\gamma_{bi} z} \boldsymbol{u}_z \times \boldsymbol{e}_{bi} \tag{2b}$$

with B_i and G_i as the respective coefficients of the reflected modes and the modes produced by $-\boldsymbol{M}$. The last term in (1) and (2) corresponds to the fields generated by the equivalent magnetic current $\boldsymbol{M}$ (i.e., at $z = 0$ the first two terms cancel each other). γ_{qi} is the mode propagation constant and Y_{qi} is the modal characteristic admittance in the waveguide and in the crack $q \in \{a, b\}$ [2].

B. Forcing the Boundary Conditions

For a general case as shown in Fig. 1, the transverse electric fields have to vanish at the short-circuited end of the crack $z = d$, it follows that

$$G_i = B_i \left[e^{2\gamma_{bi} d} - 1 \right]. \tag{3}$$

Next, the continuity of the transverse electric field $\boldsymbol{E}_t$ across the aperture S has to be satisfied. The placement of an equivalent magnetic current density $+\boldsymbol{M}$ across the aperture S in the waveguide and $-\boldsymbol{M}$ across S in the crack ensures the continuity of $\boldsymbol{E}_t$ across S. The equivalent magnetic current density $\boldsymbol{M}$ can hence be evaluated from (1) and (2) as

$$\boldsymbol{M} = \boldsymbol{u}_z \times \boldsymbol{E}_{at} \,|_{z=0} = \sum_i D_i \boldsymbol{u}_z \times \boldsymbol{e}_{ai} \tag{4a}$$

and

$$\boldsymbol{M} = \boldsymbol{u}_z \times \boldsymbol{E}_{bt} \,|_{z=0} = \sum_i B_i \left[e^{2\gamma_{bi} d} - 1 \right] \boldsymbol{u}_z \times \boldsymbol{e}_{bi}. \tag{4b}$$

Likewise, the continuity of $\boldsymbol{H}_t$ across the aperture S requires that

$$2 \sum_i C_i Y_{ai} \boldsymbol{u}_z \times \boldsymbol{e}_{ai} = \sum_i D_i Y_{ai} \boldsymbol{u}_z \times \boldsymbol{e}_{ai} + \sum_i B_i Y_{bi} \left[e^{2\gamma_{bi} d} + 1 \right] \boldsymbol{u}_z \times \boldsymbol{e}_{bi}. \tag{5}$$

In order to obtain a numerical solution of (5), the method of moments is applied [17].

C. Application of the Method of Moments

$\boldsymbol{M}$ is first expanded as a complete set of basis functions, $\boldsymbol{M}_j$, which consists of N real valued expansion functions and V_j are complex variables which are unknown and to be determined. These basis functions, which describe the behavior of the magnetic field right at the aperture, will have to be chosen appropriately for obtaining a close-to-the-exact solution and to achieve fast convergence. If the number of modes in the waveguide is limited to L_a and the number of modes in the crack to L_b, and N expansion functions are used, then

$$\sum_{j=1}^{N} V_j \boldsymbol{M}_j = \sum_{i=1}^{L_a} D_i \boldsymbol{u}_z \times \boldsymbol{e}_{ai} \tag{6a}$$

$$\sum_{j=1}^{N} V_j \boldsymbol{M}_j = \sum_{i=1}^{L_b} B_i \left[e^{2\gamma_{bi} d} + 1 \right] \boldsymbol{u}_z \times \boldsymbol{e}_{bi}. \tag{6b}$$

Now, by using orthogonality of mode vectors, and by scalarly multiplying (6a) and (6b) by $\boldsymbol{u}_z \times \boldsymbol{e}_{ak}$ and $\boldsymbol{u}_z \times \boldsymbol{e}_{bk}$, respectively, and then integrating over the corresponding waveguide and crack aperture surfaces S_a and S_b, the following equations are obtained:

$$D_i = \sum_{j=1}^{N} V_j H_{aij}, \qquad i = 1, 2, \ldots, L_a \tag{7a}$$

$$B_i = \left(\sum_{j=1}^{N} V_j H_{bij} \right) \left[e^{2\gamma_{bi} d} - 1 \right]^{-1}, \qquad i = 1, 2, \ldots, L_b \tag{7b}$$

where

$$H_{aij} = \iint_{S_a} \boldsymbol{M}_j \cdot \boldsymbol{u}_z \times \boldsymbol{e}_{ai}\, dS_a \tag{8a}$$

$$H_{bij} = \iint_{S_b} \boldsymbol{M}_j \cdot \boldsymbol{u}_z \times \boldsymbol{e}_{bi}\, dS_b. \tag{8b}$$

Using Galerkin's method, and forming the scalar product of (5) with each of the testing functions $\boldsymbol{M}_k$ gives

$$2\sum_{i=1}^{L_a} C_i Y_{ai} P_{aik} = \sum_{i=1}^{L_a} D_i Y_{ai} P_{aik} + \sum_{i=1}^{L_b} B_i Y_{bi} \left[e^{2\gamma_{bi} d} + 1\right] P_{bik} \tag{9}$$

where

$$P_{aik} = \iint_{S_a} \boldsymbol{M}_k \cdot \boldsymbol{u}_z \times \boldsymbol{e}_{ai}\, dS_a \tag{10a}$$

$$P_{bik} = \iint_{S_b} \boldsymbol{M}_k \cdot \boldsymbol{u}_z \times \boldsymbol{e}_{bi}\, dS_b. \tag{10b}$$

After substitution for D_i and B_i from (7), (11) is shown at bottom of the page.

D. Matrix Form

Equation (11) is now written in a matrix form as

$$\vec{\boldsymbol{I}} = [\bar{\boldsymbol{Y}}_a + \bar{\boldsymbol{Y}}_b]\vec{V} \tag{12}$$

where

$$\vec{\boldsymbol{I}} = 2\boldsymbol{P}_a^T \boldsymbol{Y}_a \vec{C} \tag{13a}$$

$$\bar{\boldsymbol{Y}}_a = \boldsymbol{P}_a^T \boldsymbol{Y}_a \boldsymbol{H}_a \tag{13b}$$

$$\bar{\boldsymbol{Y}}_b = \boldsymbol{P}_b^T \boldsymbol{Y}_b \boldsymbol{E}_1 \boldsymbol{E}_2 \boldsymbol{H}_b. \tag{13c}$$

$\boldsymbol{Y}_a$, $\boldsymbol{Y}_b$, $\boldsymbol{E}_1$, and $\boldsymbol{E}_2$ are diagonal matrices whose elements are readily evaluated. Note that $\boldsymbol{P}_a^T = \boldsymbol{H}_a^T$ and $\boldsymbol{P}_b^T = \boldsymbol{H}_b^T$ when using the Galerkin's method.

E. Generalized Scattering Matrix

Now it is possible to evaluate the generalized scattering matrix $\boldsymbol{S}$ of the waveguide-crack junction. From (1) the reflected wave is given by

$$\vec{A} = \vec{D} - \vec{C}. \tag{14}$$

Substituting for $\vec{D}$ and evaluating $\vec{V}$ from (12) gives

$$\vec{D} = \boldsymbol{H}_a \vec{V} = \boldsymbol{H}_a 2[\bar{\boldsymbol{Y}}_a + \bar{\boldsymbol{Y}}_b]^{-1} \boldsymbol{P}_a^T \boldsymbol{Y}_a \vec{C}. \tag{15}$$

Then, (14) is rewritten as

$$\vec{A} = \left[2\boldsymbol{H}_a[\bar{\boldsymbol{Y}}_a + \bar{\boldsymbol{Y}}_b]^{-1} \boldsymbol{P}_a^T \boldsymbol{Y}_a - \boldsymbol{U}\right]\vec{C} \tag{16}$$

where $\boldsymbol{U}$ is the unity matrix. Subsequently, $\boldsymbol{S}_{aa}$ is expressed as

$$\boldsymbol{S}_{aa} = \vec{A}\vec{C}^{-1} = 2\boldsymbol{H}_a[\bar{\boldsymbol{Y}}_a + \bar{\boldsymbol{Y}}_b]^{-1} \boldsymbol{P}_a^T \boldsymbol{Y}_a - \boldsymbol{U}. \tag{17}$$

Note that S_{ij} is the amplitude of the ith mode due to the jth incident mode with unit amplitude. Here, the authors are not concerned with $\boldsymbol{S}_{ba}$, $\boldsymbol{S}_{ab}$, and $\boldsymbol{S}_{bb}$, which are the other scattering coefficients in the waveguide and the crack. However, if need be, they can be readily calculated as well.

In order to calculate the *crack characteristic signal*, it is necessary to evaluate the submatrix $\boldsymbol{S}_{aa}$ (reflection coefficient of the dominant mode and each of the higher order modes) of the generalized scattering matrix $\boldsymbol{S}$ for different positions of the crack relative to the waveguide aperture. Once the reflection coefficient of the incident dominant TE_{10} mode is known, the shift of the standing wave in the waveguide can be evaluated. Subsequently, the diode output voltage (probing the standing wave) for the dominant mode detection technique can be computed to obtain the *crack characteristic signal* [3].

IV. Convergence

A. Choice of Basis Functions

The above moment solution approach and the subsequent generalized scattering parameters depend on the choice of an initially unknown equivalent magnetic current density $\boldsymbol{M}$ over a conducting surface. $\boldsymbol{M}$ is described by basis functions that form a complete set. Since $\boldsymbol{M}$ describes the physical behavior of the magnetic field over the aperture S, it is best to choose the basis functions to have similar properties to the orthonormal mode vectors of the transverse magnetic fields in the waveguide and the crack. In this way, a relatively fast convergence may be obtained. Hence, $\boldsymbol{M}$ is chosen as following

$$\boldsymbol{M}_j = \boldsymbol{u}_x \sin\left(\frac{q'\pi x}{g}\right)\cos\left(\frac{p'\pi y}{h}\right) + \boldsymbol{u}_y \cos\left(\frac{q\pi x}{g}\right)\sin\left(\frac{p\pi y}{h}\right) \tag{18}$$

where g and h are the dimensions of the aperture opening S (Fig. 1). It must be noted that q' and p cannot equal zero. This is obvious from the fact that TE_{0m} and TE_{n0} modes exist, but not TM_{0m} or TM_{n0} modes.

The rate of convergence is critically dependent on the number of basis functions used to describe $\boldsymbol{M}$. Fig. 2 shows that faster convergence is achieved when the maximal indices in x- and y-direction are chosen to be the same ($q'_{\max} = q_{\max}$ and $p'_{\max} = p_{\max}$). The normalized signal (i.e., the diode output voltage representing one sample of the *crack characteristic signal*) is calculated and plotted for an increasing number of

$$2\sum_{i=1}^{L_a} C_i Y_{ai} P_{aik} = \sum_{i=1}^{L_a} \left(\sum_{j=1}^{N} V_j H_{aij}\right) Y_{ai} P_{aik} + \sum_{i=1}^{L_b} \left(\sum_{j=1}^{N} V_j H_{bij}\right) \frac{\left[e^{2\gamma_{bi} d} + 1\right]}{\left[e^{2\gamma_{bi} d} - 1\right]} Y_{bi} P_{bik} \tag{11}$$

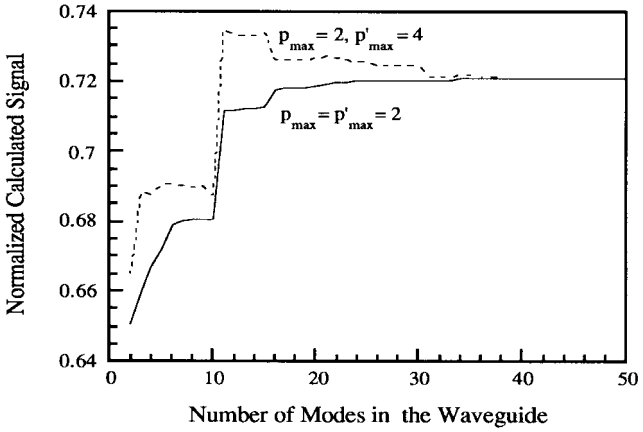

Fig. 2. Convergence curves for a long crack with a width of 0.84 mm and a depth of 1.53 mm at 24 GHz, at the relative coordinates ($x = 0$ mm, $y = -0.4$ mm), with different combinations of basis functions in x- and y-directions.

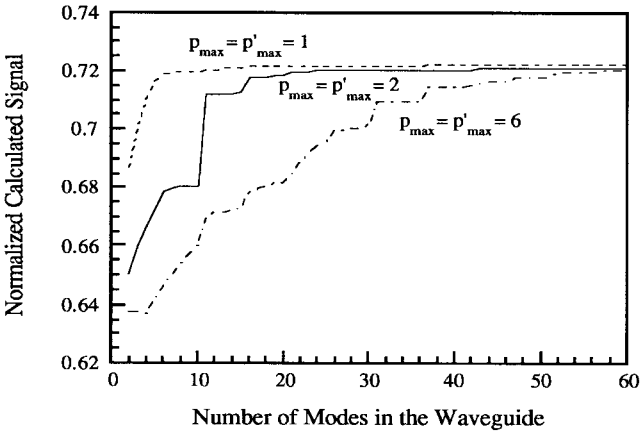

Fig. 3. Relative convergence problem for a long crack with a width of 0.84 mm and a depth of 1.53 mm at 24 GHz, at the relative coordinates ($x = 0$ mm, $y = -0.4$ mm), with increasing numbers of basis functions in x- and y-directions.

modes in the waveguide for a crack at the relative coordinates ($x = 0, y = -0.4$). For simplicity, a crack with its length equal to the broad dimension of the waveguide is considered. Thus, only TE_{1m} and TM_{1m} modes have to be considered, and $q'_{\max} = q_{\max} = 1$, as no variation in the x-direction is encountered [3]. The number of modes in the crack is chosen proportional to the number of modes in the waveguide by the ratio of w over b. In the case of $p'_{\max} = p_{\max} = 2$, the final value for the diode output voltage is achieved with 22 modes in the waveguide compared to 36 modes for $p'_{\max} = 4, p_{\max} = 2$, when allowing an error of 0.1%. Moreover, the overshooting effect as seen in Fig. 2 for $p'_{\max} \neq p_{\max}$ is avoided. Allowing a larger error with respect to the final value would further significantly reduce the number of modes needed in the calculations.

In the case that the number of basis functions used to describe the magnetic current density $\boldsymbol{M}$ is not sufficient, the problem of relative convergence is encountered [22]. Fig. 3 shows the convergence curves for increasing numbers of basis functions. It is seen that once a sufficient number of basis functions is used, the signal amplitude of the *crack characteristic signal* does not change significantly (0.22% error for $p'_{\max} = p_{\max} = 1$, and 0.054% error for $p'_{\max} = p_{\max} = 2$). Increasing the number of basis functions further reduces the speed of convergence. Thus, for an error of less than 0.1%, 22 modes are needed in the waveguide for $p'_{\max} = p_{\max} = 2$ versus 56 modes for $p'_{\max} = p_{\max} = 6$. Clearly, a minimal number of basis functions is desired for reducing the computation time while achieving accurate results.

The optimal number of basis functions depends on the physical dimensions of the waveguide (a and b) and the crack (i.e., length ℓ and width w), as well as the size of the aperture S (with dimensions g and h, which change as a function of the relative crack location within the waveguide aperture). Through extensive numerical evaluations the following criteria have been established for choosing an appropriate number of basis functions:

$$q'_{\max} = q_{\max} = \mathrm{ceil}\left(\frac{\ell}{g}\right) + 1 \leq 5 \tag{19a}$$

$$p'_{\max} = p_{\max} = \mathrm{ceil}\left(\frac{w}{h}\right) + 1 \leq 5. \tag{19b}$$

The operator (ceil) means rounding off to the larger integer. For achieving fast convergence with the method of moments it is best to approximate the actual physical behavior of the magnetic field over the aperture. In order to accommodate for the magnetic field at the edges of the aperture a different set of basis functions may be applied. For this case $\boldsymbol{M}$ is defined by

$$\boldsymbol{M}_j = \boldsymbol{u}_x \frac{\sin\left(\frac{q'\pi x}{g}\right)\cos\left(\frac{p'\pi y}{h}\right)}{\sqrt{1-\alpha\left(\frac{y-\frac{h}{2}}{\frac{h}{2}}\right)}} + \boldsymbol{u}_y \cos\left(\frac{q\pi x}{g}\right)\sin\left(\frac{p\pi y}{h}\right) \tag{20}$$

where α, a number close to one, is introduced to avoid infinity. The number of modes needed in the waveguide and the crack are not significantly reduced compared to that used in (18). On the contrary, the necessary numerical integrations for evaluating the matrix elements of H_{aij} and H_{bij} result in an overall slower computation time, and is, therefore, not considered here.

B. Choice of Higher Order Modes

Once an optimal set of the basis functions is chosen it becomes necessary to obtain a criterion for choosing an appropriate number of modes in the waveguide and in the crack. This number again depends on the physical dimensions of the waveguide, the crack, and the size of the aperture S (g and h). Since the evaluation of the *crack characteristic signal* is dependent on the position of the crack relative to the waveguide aperture, the size of the aperture S changes. When the crack is just about to enter the waveguide aperture, the aperture S is very narrow (i.e., h being very small), and a higher number of modes is needed. A thorough study of the convergence behavior for the crack at different relative positions with respect to the waveguide aperture has indicated

that the maximal indices n and m for the waveguide side are

$$n_{a\max} = \text{ceil}\left(\frac{q_{\max} a}{g}\right) \tag{21a}$$

$$m_{a\max} = \text{ceil}\left(\frac{p_{\max} b}{h}\right) \tag{21b}$$

The TE_{nm} and TM_{nm} modes are degenerate modes (modes with the same cutoff frequency) and, hence, must be considered as pairs [21]. Only in special situations it is possible to significantly reduce the number of modes used. For instance, for a long crack (i.e., the crack length is equal to the broad dimension of the waveguide) only TE_{1m} and TM_{1m} modes have to be considered as no variation in the x-direction is encountered [3]. All the coefficients of the other higher order modes would evaluate to zero in this special case.

For the number of modes in the crack a similar criterion is considered and, hence, the maximal indices $n_{b\max}$ and $m_{b\max}$ of the desired number of TE_{nm} and TM_{nm} modes in the crack are given by

$$n_{b\max} = \text{ceil}\left(\frac{q_{\max} \ell}{g}\right) \tag{22a}$$

$$m_{b\max} = \text{ceil}\left(\frac{p_{\max} w}{h}\right). \tag{22b}$$

It must be noted that when the crack is totally within the waveguide aperture ($\ell = g$ and $w = h$), the number of basis functions are identical to the number of modes in the crack. This is sufficient when $\boldsymbol{M}$ is chosen as in (18), because the basis functions over the aperture S directly correspond to the orthonormal mode vectors of the magnetic field in the crack. Thus, the fields are described in a similar fashion and the coefficients of all other higher order modes in the crack would evaluate to zero (i.e., these modes are orthogonal to the basis functions).

V. Results

A. Field Distribution

The tangential electric field E_y at the aperture of the waveguide (i.e., at $z = 0$) has been evaluated numerically. In order to show the versatility of this technique, the field is evaluated for a finite crack in the middle of the waveguide aperture. This finite crack/slot with a length of 6 mm, a width of 0.84 mm, and a depth of 1.53 mm is positioned with the corner P of the crack at the relative coordinates ($x = 2$ mm, $y = 1$ mm), and the electric field is shown in Fig. 4. As expected, the tangential electric field E_y vanishes over the conducting surfaces, whereas it has a finite value over the aperture S. In order to further reduce the ripples of the electric field visible over the conducting surfaces, more modes could be used.

B. Comparison Between Theory and Measurement

To show the validity of this theoretical approach, the calculated *crack characteristic signal* is compared with the measured *crack characteristic signal* (Fig. 5) for a long milled crack/slot with a width of 0.55 mm and a depth of 2.5 mm at 24 GHz. The measured *crack characteristic signal* was normalized with respect to its short-circuit value (crack outside the waveguide aperture). The agreement between the calculated and measured *crack characteristic signal* is very good. The slight deviations are due to a limited number of modes used in the calculation, imperfection in machining a crack on a metal surface as specified in the calculations as well as the detector diode characteristics.

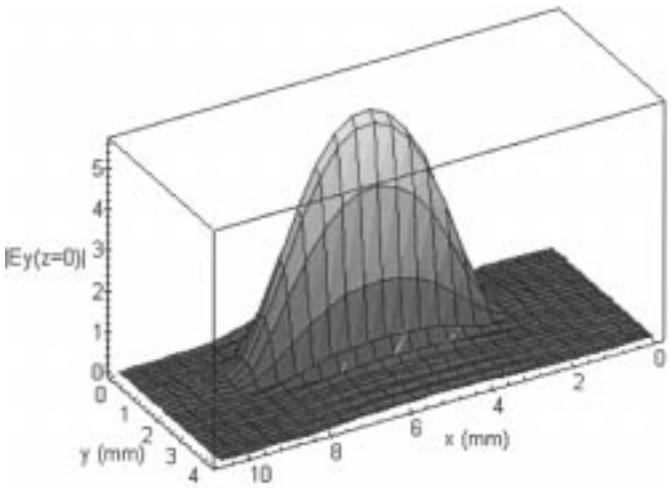

Fig. 4. Tangential electric field E_y at the waveguide aperture (i.e., $z = 0$) for a finite crack with a length of 6 mm, a width of 0.84 mm, and a depth of 1.53 mm at 24 GHz, at the relative coordinates ($x = 2.5$ mm, $y = 1$ mm).

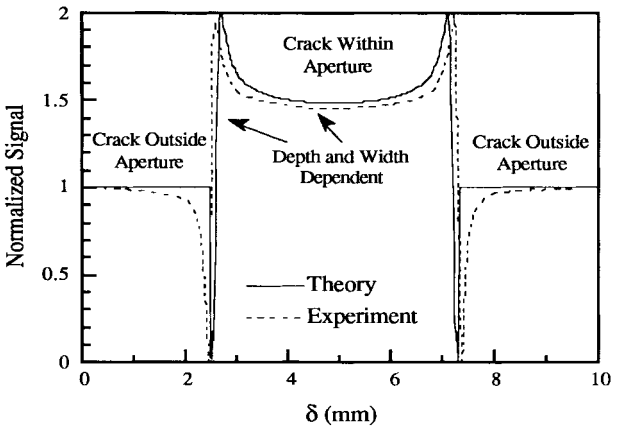

Fig. 5. *Crack characteristic signal* for a long crack with a width of 0.55 mm and a depth of 2.5 mm at 24 GHz: calculated (—-) and measured (- - -).

C. Crack Characteristic Signal for Filled Crack

The properties of the *crack characteristic signal* are a function of the crack width, depth, and length [14]. When the crack is filled with a dielectric material its *crack characteristic signal* also changes compared to the case when it is empty. Fig. 6 shows the normalized calculated and measured *crack characteristic signal*s, recorded at a frequency of 24 GHz for empty and filled (with rust powder) (measured as $\varepsilon_r = 6.25 - j0.05$) cracks/slots, with a width of 0.85 mm and a depth of 1.25 mm, respectively. The reduction in the width of the *crack characteristic signal* (distance between the two sharp transitions) and the change in the middle level of the *crack characteristic signal* are evident, as experimentally investigated further in [2]. This

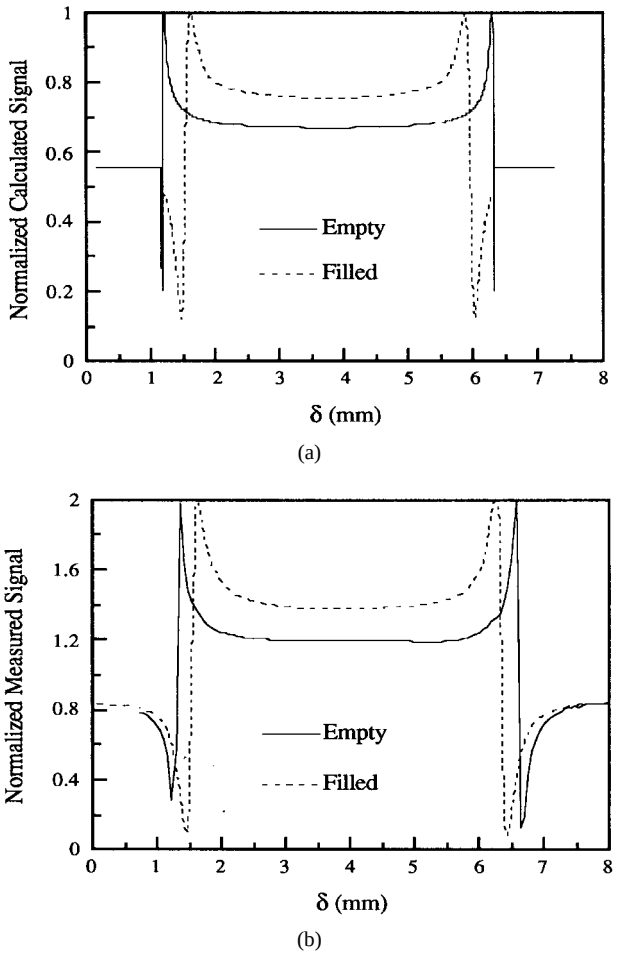

Fig. 6. Normalized *crack characteristic signal* for an empty and filled (with rust powder) crack with a width of 0.85 mm and a depth of 1.25 mm at a frequency of 24 GHz: (a) calculated, (b) measured.

method may also be used in tandem with other nondestructive testing (NDT) techniques (dye penetrant) for optimizing depth determination of shallow cracks.

VI. Conclusion

The evaluation of the electromagnetic properties in a system formed by a waveguide and a surface crack in a metallic specimen has been demonstrated. A moment solution approach is employed to express the reflection coefficient for this system in terms of the generalized scattering matrix for an arbitrary incident field. The evaluation of the generalized scattering matrix employs the equivalence principle and a moment solution approach. This approach is proven to be a powerful technique for theoretically evaluating the electromagnetic properties for empty, filled, or finite cracks, independent of the position relative to the waveguide aperture. Thus, compared to a previously developed mode-matching approach, this method is more flexible and simultaneously reduces the computational time. So it becomes possible to implement this approach on a PC. The field distribution of the tangential electric field E_y is evaluated at the waveguide aperture to check the boundary conditions. Further, the theoretical *crack characteristic signal* for a long crack is evaluated and compared to an experimental result. The agreement between the two is very good. The change in the *crack characteristic signal* for an empty and a filled crack is also investigated. The *crack characteristic signal* for very tight cracks can be calculated at higher frequencies. With the given computer resources (i.e., Pentium with 64 MB RAM) it is possible to evaluate hairline cracks with widths less than 0.085 mm at 65 GHz (not shown here). In addition, this approach is useful in expanding upon and encompassing the evaluation of covered cracks.

References

[1] K. G. Boving, *NDE Handbook, Non-Destructive Examination Methods for Condition Monitoring*. London, U.K.: Butterworths, 1989.
[2] C. Huber, "Electromagnetic modeling of exposed and covered surface crack detection using open-ended waveguides," Ph.D. dissertation, Elec. Eng. Dept., Colorado State Univ., Fort Collins, CO, 1996.
[3] C. Yeh and R. Zoughi, "A novel microwave method for detection of long surface cracks in metals," *IEEE Trans. Instrum. Meas.*, vol. 43, pp. 719–725, Oct. 1994.
[4] C. Yeh, "Detection and sizing of surface cracks in metals using open-ended rectangular waveguides," Ph.D. dissertation, Elec. Eng. Dept., Colorado State Univ., Fort Collins, CO, May 1994.
[5] L. Feinstein and R. J. Hrby, "Surface crack detection by microwave methods," presented at the 6th Symp. Nondestructive Evaluation Aerospace Weapons Sys. Components and Materials, San Antonio, TX, 1967.
[6] A. J. Bahr, "Microwave eddy-current techniques for quantitative non-destructive evaluation," in *Eddy-Current Characterization of Materials and Structures*, G. Birnbaum and G. Free, Eds., ASTM STP 722, pp. 311–331, 1981.
[7] L. A. Robinson and U. H. Gysel, "Microwave coupled surface crack detector," Stanford Res. Inst., Menlo Park, CA, Contract DAAG-46-72-C-0019, SRI Project 1490, Aug. 1972.
[8] A. Husain and E. A. Ash, "Microwave scanning microscopy for non-destructive testing," in *Proc. 5th European Microwave Conf.*, Hamburg, Germany, Sept. 1975, pp. 213–217.
[9] B. A. Auld, "Theory of ferromagnetic resonance probes for surface cracks in metals," E. L. Ginzton Lab., Stanford Univ., Stanford, CA, G. L. Rep. 2839, July 1978.
[10] C. Yeh, E. Ranu, and R. Zoughi, "A novel microwave method for surface crack detection using higher order waveguide modes," *Mat. Eval.*, vol. 52, no. 6, pp. 676–681, June 1994.
[11] C. Yeh and R. Zoughi, "Sizing technique for surface cracks in metals," *Mat. Eval.*, vol. 53, no. 4, pp. 496–501, Apr. 1995.
[12] ——, "Microwave detection of finite surface cracks in metals using rectangular waveguide sensors," *Res. in Nondestructive Evaluation*, vol. 6, no. 1, pp. 35–55, 1994.
[13] S. Ganchev, R. Zoughi, C. Huber, R. Runser, and E. Ranu, "Microwave method for locating surface crack tips in metals," *Mat. Eval.*, vol. 54, no. 5, pp. 598–603, May 1996.
[14] R. Zoughi, S. I. Ganchev, C. Huber, E. Ranu, and R. Runser, "A novel microwave method for filled and covered surface crack detection in steel bridge members including crack tip identification," Federal Highway Administration, McLean, VA, Fourth Quart. Rep., Contract DTFH61-94-X-00023, Sept. 1995.
[15] H. Auda and R. F. Harrington, "A moment solution for waveguide junction problems," *IEEE Trans. Microwave Theory Tech.*, vol. MTT-31, pp. 515–519, July 1983.
[16] R. F. Harrington, *Time Harmonic Electromagnetic Fields*. New York: McGraw-Hill, 1961.
[17] R. F. Harrington, *Field Computation by Moment Methods*. New York: MacMillan, 1968.
[18] R. F. Harrington and J. R. Mautz, "A generalized network formulation for aperture problems," *IEEE Trans. Antennas Propagat.*, vol. AP-24, pp. 870–873, Nov. 1976.
[19] F. E. Borgnis and C. H. Papas, *Encyclopedia of Physics: Electromagnetic Waveguides and Resonators*. Berlin, Germany: Springer-Verlag, vol. XVI, 1958.
[20] N. Marcuvitz, *Waveguide Handbook*. New York: McGraw-Hill, 1951.
[21] R. E. Collin, *Foundations for Microwave Engineering*. New York: McGraw-Hill, 1992.
[22] J. Uher, J. Bornemann, and U. Rosenberg, *Waveguide Components for Antenna Feed Systems: Theory and CAD*. Norwood, MA: Artech House, 1993.

Christian Huber received the Dipl.-Ing. degree from the Technical University of Vienna, Austria, and the Ph.D. degree from Colorado State University, Fort Collins, in 1992 and 1995, respectively.

His research at the Applied Microwave Nondestructive Testing Laboratory (*amntl*), Department of Electrical Engineering, Colorado State University, Fort Collins, was on surface-crack detection using open-ended waveguides. Presently, he is a Post-Doctoral Fellow at the same laboratory, continuing his research efforts on nondestructive surface inspection of metals using microwaves.

Habibollah Abiri, photograph and biography not available at time of publication.

Stoyan I. Ganchev (M'92–SM'92) received the M.Sc. degree in physics from the University of Sofia, Sofia, Bulgaria, and Ph.D. degree from the Institute of Electronics, Bulgarian Academy of Sciences, Sofia, Bulgaria, in 1969 and 1985, respectively.

From 1969 to 1990, he was engaged in research on microwave ferrites and ferrite devices at the Institute of Electronics. He is the Senior Research Associate at the Applied Microwave Nondestructive Testing Laboratory (*amntl*), Department of Electrical Engineering, Colorado State University, Fort Collins. His current research interest is microwave nondestructive evaluation and he has published extensively in this area.

Reza Zoughi (S'85–M'86–SM'93) received the B.S.E.E, M.S.E.E, and Ph.D. degrees in electrical engineering (radar remote sensing, radar systems, and microwaves) from the University of Kansas, Lawrence, in 1982, 1983, and 1987, respectively.

From 1981 to 1987 he was employed by the Radar Systems and Remote Sensing Laboratory (RSL), University of Kansas, in various capacities. His experience at RSL included developing, building, and operating various radar systems, data collection, and analysis. He has been at Colorado State University, Fort Collins, since 1987, and he is currently an Associate Professor in the Electrical Engineering Department where he established the Applied Microwave Nondestructive Testing Laboratory. He is an Associate Technical Editor for Materials Evaluation and served as the Guest Associate Editor for the Special Microwave NDE Issue of Research in Nondestructive Evaluation in 1995. He has published over 150 publications, conference proceedings, and technical reports. His current areas of research include nondestructive testing of material using microwaves, developing new techniques for microwave and millimeter-wave inspection, and testing of materials and developing new electromagnetic probes to measure characteristic properties of material at microwave frequencies. He has been voted the most outstanding teaching faculty for the past six years by the junior and senior students, Electrical Engineering Department, Colorado State University. He has also been recognized as an honored researcher by the Colorado State University Research Foundation.

Dr. Zoughi is the recipient of the Dean's Council Award in 1992, and the Abell Faculty Teaching Award in 1995. He is also the Business Challenge Endowment Associate Professor of Electrical Engineering (1995–1997) and the 1996 recipient of the Colorado State Board of Agriculture Excellence in Undergraduate Teaching Award. He is a member of Sigma Xi, Eta Kappa Nu and the American Society for Nondestructive Testing (ASNT).